INTERNATIONAL JOURNAL FOR NUMERICAL METHODS IN FLUIDS, VOL. 8, 441–461 (1988)

ON THE SMOOTHING PROPERTIES OF THE SIMPLE PRESSURE-CORRECTION ALGORITHM

G. J. SHAW AND S. SIVALOGANATHAN

Oxford University Computing Laboratory, 8–11 Keble Rd, Oxford, U.K.

SUMMARY

A local mode Fourier analysis is used to assess the suitability of the SIMPLE pressure-correction algorithm to act as a smoother in a multigrid method. The necessary ellipticity of the Navier–Stokes equations and their discrete representation are established. The theoretical analysis is compared with practical results.

KEY WORDS Multigrid Local mode analysis Pressure correction Ellipticity

INTRODUCTION

In a companion paper Sivaloganathan and Shaw[1] present an efficient non-linear multigrid procedure for the incompressible Navier–Stokes equations. The underlying smoothing method used is the SIMPLE pressure-correction algorithm of Patankar and Spalding.[2] It is found empirically that this method has satisfactory smoothing properties over a wide range of Reynolds numbers. The method reduces high-frequency error components sufficiently to enable the construction of a multigrid method which exhibits grid-independent convergence rates.

The aim of the present paper is to confirm these results by means of a Fourier analysis of the SIMPLE algorithm. Such an analysis is justified in the context of a multigrid smoother, since we are interested only in the high-frequency error reduction and these errors have a small domain of influence. The analysis presented in this paper is readily extended to include other pressure-correction methods such as SIMPLER and SIMPLEST.

The existence of iterative methods with good error-smoothing properties depends upon the ellipticity of the discrete representation of the partial differential equations in question. This in turn is dependent on the ellipticity of the continuous system. For this reason the paper begins by establishing that both the incompressible Navier–Stokes equations and their discretization—as described in Sivaloganathan and Shaw[1]—are elliptic.

It is found that the practical behaviour of the iteration is well modelled by Fourier analysis and that the SIMPLE algorithm has good smoothing properties.

CONTINUOUS AND DISCRETE ELLIPTICITY

In this section we establish the ellipticity of the continuous and discrete systems of equations under consideration. Ellipticity of the continuous system is meant in the sense of Douglis and Nirenberg,[3] while the definition of Thomée[4] motivates the application to the discrete approximation.

Brandt and Dinar[5] generalize this concept of discrete ellipticity and discuss its importance in the

0271–2091/88/040441–21$10.50

Received 1 March 1987

Fourier analysis of smoothing methods. Their approach is followed in this paper. As illustrated by Shaw,[6] the discrete ellipticity of a discretization is a necessary condition for the existence of a smoothing method.

Continuous ellipticity

The Navier–Stokes equations for the steady incompressible flow of a Newtonian gas may be written as

$$\frac{\partial \rho u^2}{\partial x}+\frac{\partial \rho uv}{\partial y}+\frac{\partial p}{\partial x}-\frac{\partial}{\partial x}\left(2\mu\frac{\partial u}{\partial x}\right)-\frac{\partial}{\partial y}\left[\mu\left(\frac{\partial u}{\partial y}+\frac{\partial v}{\partial x}\right)\right]=0, \tag{1a}$$

$$\frac{\partial \rho v^2}{\partial y}+\frac{\partial \rho uv}{\partial x}+\frac{\partial p}{\partial y}-\frac{\partial}{\partial y}\left(2\mu\frac{\partial v}{\partial y}\right)-\frac{\partial}{\partial x}\left[\mu\left(\frac{\partial u}{\partial y}+\frac{\partial v}{\partial x}\right)\right]=0, \tag{1b}$$

$$\frac{\partial \rho u}{\partial x}+\frac{\partial \rho v}{\partial y}=0, \tag{1c}$$

where x, y denote the co-ordinate axes and u, v the components of the velocity in these directions; p denotes the static pressure, ρ the density and μ the viscosity; ρ and μ are assumed to be given functions of x, y only.

A linearization of (1) is obtained by freezing ρ, μ at ρ_0, μ_0 respectively, and velocities u, v, where they contribute to non-linear terms, at u_0, v_0 respectively. For simplicity it is assumed that ρ_0, μ_0, u_0, v_0 are constants. The linearized system may then be written as

$$\begin{bmatrix} c-\mu_0\left(2\dfrac{\partial^2}{\partial x^2}+\dfrac{\partial^2}{\partial y^2}\right) & -\mu_0\dfrac{\partial^2}{\partial x\,\partial y} & \dfrac{\partial}{\partial x} \\ -\mu_0\dfrac{\partial^2}{\partial x\,\partial y} & c-\mu_0\left(2\dfrac{\partial^2}{\partial y^2}+\dfrac{\partial^2}{\partial x^2}\right) & \dfrac{\partial}{\partial y} \\ \dfrac{\partial}{\partial x} & \dfrac{\partial}{\partial y} & 0 \end{bmatrix}\begin{bmatrix} u \\ v \\ p \end{bmatrix}=\begin{bmatrix} 0 \\ 0 \\ 0 \end{bmatrix}, \tag{2}$$

where the linearized convective operator

$$c=\rho_0\left(u_0\frac{\partial}{\partial x}+v_0\frac{\partial}{\partial y}\right). \tag{3}$$

For the purposes of this paper, non-linear systems of equations will be considered to be elliptic if the linearized equations are elliptic for any choice of the frozen values ρ_0, μ_0, u_0, v_0. For brevity we denote system (2) as

$$\mathbf{Lq}=\mathbf{0}, \tag{4}$$

where $\mathbf{L}$ is a linear operator and $\mathbf{q}=(u,v,p)^{\mathrm{T}}$ is a state vector. The Fourier transform $\hat{\mathbf{L}}$ of $\mathbf{L}$ is given by

$$\hat{\mathbf{L}}=\begin{bmatrix} \hat{c}+\mu_0(2\theta_1^2+\theta_2^2) & \mu_0\theta_1\theta_2 & \mathrm{i}\theta_1 \\ \mu_0\theta_1\theta_2 & \hat{c}+\mu_0(2\theta_2^2+\theta_1^2) & \mathrm{i}\theta_2 \\ \mathrm{i}\theta_1 & \mathrm{i}\theta_2 & 0 \end{bmatrix}, \tag{5}$$

where $\hat{c}=\rho_0\mathrm{i}(u_0\theta_1+v_0\theta_2)$ is the Fourier transform of c from (x,y) into (θ_1,θ_2). $\hat{L}$ is known as the symbol of L.

Ellipticity of (1) in the sense of Douglis and Nirenberg[3] depends on the regularity of $\hat{\mathbf{L}}$ for $\boldsymbol{\theta} = (\theta_1, \theta_2)^{\mathrm{T}}$ not equal to 0. To investigate the ellipticity of the system, we consider the determinant $\tilde{L}$ of $\hat{\mathbf{L}}$:

$$\tilde{L} = \det \hat{\mathbf{L}} = (\theta_1^2 + \theta_2^2)[\mu_0(\theta_1^2 + \theta_2^2) + \rho_0 \mathrm{i}(u_0\theta_1 + v_0\theta_2)]. \tag{6}$$

The system (4) is defined to be elliptic if $\tilde{L}$ is non-zero for all real $\boldsymbol{\theta}$ not equal to 0. Clearly this is the case for all non-zero μ_0 and hence the linearized problem (2) is elliptic. Thus the non-linear problem (1) is considered also to be elliptic.

Defining the Reynolds number as $Re = \rho_0(u_0^2 + v_0^2)^{1/2}/\mu_0$, we note that for highly convective regimes, for which the Reynolds number is large, ellipticity is most nearly lost for lines in the (θ_1, θ_2) plane perpendicular to a local streamline.

Discrete ellipticity

In this section we demonstrate the ellipticity of the discretization of equations (1) described by Sivaloganathan and Shaw.[1] Before doing so we define discrete ellipticity in the sense of Thomée[4] and Brandt and Dinar.[5]

Symbols and ellipticity measures of Toeplitz operators

Consider the discretization of a constant-coefficient linear partial differential equation on a regular two-dimensional infinite grid of mesh length h. This yields an infinite-order banded matrix $\mathbf{L}_h$ with constant elements. Matrices of this type are termed 'Toeplitz' matrices (see Hemker[7]).

Let $\mathbf{L}_h$ be a Toeplitz matrix. The symbol $\hat{\mathbf{L}}_h(\boldsymbol{\theta})$ of $\mathbf{L}_h$ is defined by

$$\mathbf{L}_h \exp(\mathrm{i}\boldsymbol{\theta}\cdot\mathbf{x}/h) = \hat{L}_h(\boldsymbol{\theta}) \exp(\mathrm{i}\boldsymbol{\theta}\cdot\mathbf{x}/h), \tag{7}$$

where $\boldsymbol{\theta} = (\theta_1, \theta_2) \in \mathbb{R}^2$ and $\boldsymbol{\theta}\cdot\mathbf{x}/h = (\theta_1 x + \theta_2 y)/h$; hence $\hat{\mathbf{L}}_h(\theta)$ is the discrete Fourier transform of $\mathbf{L}_h$.

Thomée[4] defines $\mathbf{L}_h$ to be elliptic if $\hat{\mathbf{L}}_h(\boldsymbol{\theta}) > 0$ and also gives a stronger definition which ensures consistency of the discrete approximation. Brandt and Dinar[5] point out that formally elliptic discretizations may behave very badly for particular values of the step length h. This observation motivates the following definitions.

The 'h-ellipticity measure' of a Toeplitz matrix $\mathbf{L}_h$ is defined to be

$$E_h(\mathbf{L}_h) = \inf_{\theta \in \mathscr{H}} \frac{|\hat{\mathbf{L}}_h(\boldsymbol{\theta})|}{|\mathbf{L}_h|}, \tag{8}$$

where

$$|\mathbf{L}_h| = \sup_{\theta \in \mathscr{F}} |\hat{\mathbf{L}}_h(\boldsymbol{\theta})|, \tag{9}$$

$\mathscr{F} = [-\pi, \pi]^2$ is the set of all Fourier frequencies and $\mathscr{H} = \mathscr{F}/(-\pi/2, \pi/2)^2$ is the set of 'high' frequencies.

The Toeplitz operator $\mathbf{L}_h$ is said to be h-elliptic if $E_h(\mathbf{L}_h)$ is bounded above zero.

A discretization is said to be h-elliptic if the Toeplitz operator derived by defining it on a regular infinite grid is h-elliptic.

Generalizations

(*i*) *Variable coefficients.* If the discretization has spatially variable coefficients, it is said to be h-elliptic if it is so for each set of values of the coefficients.

(*ii*) *Non-linear problems.* A non-linear discretization is said to be h-elliptic if its linearization about any solution is h-elliptic.

(*iii*) *System of equations.* For a system of s partial differential equations, the symbol is an $s \times s$ matrix. In this case one may work with the determinant of the symbol of the discrete operator.

Other definitions are possible. For details of these, and for further generalizations of the concept of discrete ellipticity, see Brandt.[8] This publication also illustrates the relationship between h-ellipticity and the familiar continuous ellipticity.

The discrete Navier–Stokes equations

Sivaloganathan and Shaw[1] described a finite volume discretization of the system (1) on a staggered MAC grid as depicted in Figure 1. In this section we investigate the ellipticity of this discretization applied to the linearized problem (2). With reference to Figure 1, the resulting discrete equations on an infinite uniform grid of mesh length h are

$$\mathbf{L}_h \mathbf{q}_h = \begin{bmatrix} a_h^u & -\mu_0 \delta_h^x \delta_h^y & \delta_h^x \\ -\mu_0 \delta_h^x \delta_h^y & a_h^v & \delta_h^y \\ \delta_h^x & \delta_h^y & 0 \end{bmatrix} \begin{bmatrix} u_h \\ v_h \\ p_h \end{bmatrix} = \begin{bmatrix} 0 \\ 0 \\ 0 \end{bmatrix}, \tag{10}$$

where u_h, v_h, p_h are grid functions approximating u, v, p on the infinite regular grid. The component operators of $\mathbf{L}_h$ are defined by equations (5)–(8) of Sivaloganathan and Shaw[1] with ρ, μ, u, v frozen at ρ_0, μ_0, u_0, v_0 respectively.

Using these definitions, the symbol $\hat{\mathbf{L}}_h(\boldsymbol{\theta})$ of $\mathbf{L}_h$ is easily found to be

$$\hat{\mathbf{L}}_h = \begin{bmatrix} \hat{a}_h^u(\boldsymbol{\theta}) & 4\mu_0 s_1 s_2/h^2 & 2\mathrm{i}s_1/h \\ 4\mu_0 s_1 s_2/h^2 & \hat{a}_h^v(\boldsymbol{\theta}) & 2\mathrm{i}s_2/h \\ 2\mathrm{i}s_1/h & 2\mathrm{i}s_2/h & 0 \end{bmatrix}, \tag{11}$$

where

$$\hat{a}_h^u(\boldsymbol{\theta}) = \frac{4s_1^2}{h} \max\left(\frac{2\mu_0}{h}, \frac{1}{2}|\rho_0 u_0|\right) + \frac{4s_2^2}{h} \max\left(\frac{\mu_0}{h}, \frac{1}{2}|\rho_0 v_0|\right)$$

$$- \mathrm{i}\frac{\rho_0}{h}(u_0 \sin\theta_1 + v_0 \sin\theta_2), \tag{12}$$

$$\hat{a}_h^v(\boldsymbol{\theta}) = \frac{4s_2^2}{h} \max\left(\frac{2\mu_0}{h}, \frac{1}{2}|\rho_0 v_0|\right) + \frac{4s_1^2}{h} \max\left(\frac{\mu_0}{h}, \frac{1}{2}|\rho_0 u_0|\right)$$

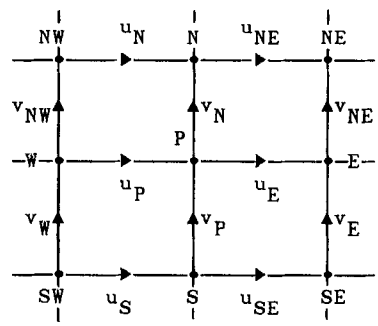

Figure 1. Staggered MAC grid

$$-\mathrm{i}\frac{\rho_0}{h}(u_0 \sin\theta_1 + v_0 \sin\theta_2), \tag{13}$$

$$s_1 = \sin(\theta_1/2), \qquad s_2 = \sin(\theta_2/2).$$

The determinant $\tilde{L}_h(\boldsymbol{\theta})$ of $\hat{\mathbf{L}}_h(\boldsymbol{\theta})$ is therefore

$$\tilde{L}_h(\boldsymbol{\theta}) = 4[s_2^2 \hat{a}_h^u(\boldsymbol{\theta}) + s_1^2 \hat{a}_h^v(\boldsymbol{\theta}) - 8\mu_0 s_1^2 s_2^2/h^2]/h^2. \tag{14}$$

Thus

$$\mathrm{Im}(\tilde{L}_h(\boldsymbol{\theta})) = -4\rho_0(s_1^2 + s_2^2)(u_0 \sin\theta_1 + v_0 \sin\theta_2)/h^3, \tag{15}$$

which is zero along lines $v_0/u_0 = -\sin\theta_1/\sin\theta_2$.

Since

$$\mathrm{Re}(\hat{a}_h^u(\boldsymbol{\theta})) \geqslant 4\mu_0(2s_1^2 + s_2^2)/h^2, \tag{16}$$

$$\mathrm{Re}(\hat{a}_h^v(\boldsymbol{\theta})) \geqslant 4\mu_0(2s_2^2 + s_1^2)/h^2, \tag{17}$$

it follows that

$$\mathrm{Re}(\tilde{L}_h(\boldsymbol{\theta})) \geqslant \mu_0[4(s_1^2 + s_2^2)/h^2]^2. \tag{18}$$

Clearly $|\tilde{L}_h(\boldsymbol{\theta})|$ is small only in the region of $(\theta_1, \theta_2) = (0,0)$ and hence $\mathbf{L}_h$ has a good h-ellipticity measure and the discretization is discretely elliptic.

SMOOTHING ANALYSIS

In this section we use local mode analysis (introduced by Brandt[9]) to examine the SIMPLE pressure-correction algorithm from the point of view of its smoothing ability. The reduction of high-frequency error components is a local process dependent principally on the local difference star. Thus the analysis of this reduction need not take account of distant boundaries or varying difference stars.

One therefore considers a sequence of Toeplitz problems obtained by defining local difference stars over infinite grids (see Shaw[6]). For each problem one may determine the amplification factor $\mu(\boldsymbol{\theta})$ which is the symbol (or discrete Fourier transform) of the relevant iteration matrix. The 'smoothing factor' $\bar{\mu}$ is defined by

$$\bar{\mu} = \sup_{\boldsymbol{\theta} \in \mathscr{H}} |\mu(\boldsymbol{\theta})|, \tag{19}$$

where $\mathscr{H}$ denotes the range of high-frequency $\boldsymbol{\theta}$ values.

This smoothing factor is a measure of the worst high-frequency error reduction. The smoothing factor of the variable-coefficient problem is then defined to be the worst of these local smoothing factors. Although the arguments for this definition are somewhat vague, it is in practice a very accurate measure of the ability of a relaxation method to damp high-frequency error components. The smoothing factor may therefore be used to optimize the efficiency of a particular method or to choose between different methods.

In the case of systems of partial differential equations, $\mu(\boldsymbol{\theta})$ is a square matrix of order equal to the number of equations in the system. The definition of the smoothing factor remains the same with $|\mu(\boldsymbol{\theta})|$ replaced by $\rho(\mu(\boldsymbol{\theta}))$ (see Shaw[6]).

If the operator is non-linear, then $\bar{\mu}$ is defined to be the worst smoothing factor of the linearized problem (about any approximate solutions which may be encountered in the solution process).

Local mode analysis

Consider an arbitrary local section of the mesh with velocity and pressure distributions as shown in Figure 1.

Assume that at the start of the iteration the errors in u, v, p are given by

$$\begin{bmatrix} e^u \\ e^v \\ e^p \end{bmatrix} = \sum_{\theta} \begin{bmatrix} e^u_\theta \\ e^v_\theta \\ e^p_\theta \end{bmatrix}$$

and that the $\boldsymbol{\theta} = (\theta_1, \theta_2)$ components of the errors are defined by

$$\begin{bmatrix} e^u_\theta \\ e^v_\theta \\ e^p_\theta \end{bmatrix} = \begin{bmatrix} \alpha^u_\theta \\ \alpha^v_\theta \\ \alpha^p_\theta \end{bmatrix} \exp(\mathrm{i}\boldsymbol{\theta}\cdot\mathbf{x}/h)$$

where $\boldsymbol{\theta}\cdot\mathbf{x}/h = (\theta_1 x + \theta_2 y)/h$.

After the first stage of SIMPLE (momentum relaxations) the error amplitudes have become

$$\begin{bmatrix} e^u_\theta \\ \dot{e}^v_\theta \\ \dot{e}^p_\theta \end{bmatrix} = \begin{bmatrix} \dot{\alpha}^u_\theta \\ \dot{\alpha}^v_\theta \\ \dot{\alpha}^p_\theta \end{bmatrix} \exp(\mathrm{i}\boldsymbol{\theta}\cdot\mathbf{x}/h).$$

and after the second stage (pressure correction)

$$\begin{bmatrix} \ddot{e}^u_\theta \\ \ddot{e}^v_\theta \\ \ddot{e}^p_\theta \end{bmatrix} = \begin{bmatrix} \ddot{\alpha}^u_\theta \\ \ddot{\alpha}^v_\theta \\ \ddot{\alpha}^p_\theta \end{bmatrix} \exp(\mathrm{i}\boldsymbol{\theta}\cdot\mathbf{x}/h).$$

Our aim is to find the amplification matrix $\mathbf{A}$ which is defined by

$$\begin{bmatrix} \ddot{\alpha}^u_\theta \\ \ddot{\alpha}^v_\theta \\ \ddot{\alpha}^p_\theta \end{bmatrix} = \mathbf{A} \begin{bmatrix} \alpha^u_\theta \\ \alpha^v_\theta \\ \alpha^p_\theta \end{bmatrix} = \mathbf{A}_2\mathbf{A}_1 \begin{bmatrix} \alpha^u_\theta \\ \alpha^v_\theta \\ \alpha^p_\theta \end{bmatrix},$$

where $\mathbf{A}_1$ and $\mathbf{A}_2$ are amplification matrices for stages 1 and 2 respectively. The smoothing factor will then be given by

$$\bar{\mu} = \sup_{\theta \in \mathscr{H}} [\rho(\mathbf{A})]. \tag{20}$$

In the case of convection-dominated flows the definition

$$\bar{\mu} = \sup_{|u_0| \leqslant 1, |v_0| \leqslant 1, \theta \in \mathscr{H}} [\rho(\mathbf{A})] \tag{21}$$

may be more relevant, where u_0, v_0 are the frozen velocities used to linearize the problem. In this case u_0, v_0 are constrained in order to maintain the relevant Reynolds number.

Momentum relaxation

The u-momentum equation of (10) may be written

$$a^u_{\mathrm{P}} u_{\mathrm{P}} = a^u_{\mathrm{W}} u_{\mathrm{W}} + a^u_{\mathrm{E}} u_{\mathrm{E}} + a^u_{\mathrm{N}} u_{\mathrm{N}} + a^u_{\mathrm{S}} u_{\mathrm{S}} - (p_{\mathrm{P}} - p_{\mathrm{W}})/h + \mu_0(v_{\mathrm{N}} - v_{\mathrm{NW}} + v_{\mathrm{W}} - v_{\mathrm{P}})/h, \tag{22}$$

where the coefficients a^u_{P}, etc. are defined by equations (7) and (8) of Sivaloganathan and Shaw[1] and contain details of viscous terms. In any case except $Re = 0$ they also contain details of convective terms, based on frozen velocities u_0, v_0. We wish to analyse the effectiveness of alternating line successive over-relaxation (SOR) as a smoother applied to equation (22).

Consider firstly x-line SOR. This is developed by writing

$$a_P^u \tilde{u}_P = a_P^u u_P + r_{mom}(a_W^u \tilde{u}_W + a_E^u \tilde{u}_E + a_N^u u_N + a_S^u \tilde{u}_S - a_P^u u_P)$$
$$+ r_{mom}[\mu_0(v_N - v_{NW} + v_W - v_P)/h^2 - (p_P - p_W)/h], \tag{23}$$

where variables with the tilde above are either updated simultaneously or are already updated due to the marching direction. The parameter r_{mom} is the relaxation factor used for the momentum equations. Since the true solution satisfies (23), the equation may be written in terms of errors:

$$a_P^u \tilde{e}_P^u = a_P^u e_P^u + r_{mom}(a_W^u \tilde{e}_W^u + a_E^u \tilde{e}_E^u + a_N^u e_N^u + a_S^u \tilde{e}_S^u - a_P^u e_P^u)$$
$$+ r_{mom}[\mu_0(e_N^v - e_{NW}^v + e_W^v - e_P^v)/h^2 - (e_P^p - e_W^p)/h]. \tag{24}$$

Then, substituting for the θ components of $\tilde{e}_P^u$ and so forth, we obtain

$$\tilde{\alpha}_\theta^u\{a_P^u - r_{mom}[a_E^u \exp(i\theta_1) + a_W^u \exp(-i\theta_1) + a_S^u \exp(-i\theta_2)]\}$$
$$= \alpha_\theta^u\{a_P^u + r_{mom}[a_N^u \exp(i\theta_2) - a_P^u]\} - \frac{4r_{mom}\mu_0}{h^2}\alpha_\theta^v s_1 s_2 - \frac{2r_{mom}i}{h}\alpha_\theta^p s_1. \tag{25}$$

In the next stage (y-line SOR) we have

$$\dot{\alpha}_\theta^u\{a_P^u - r_{mom}[a_N^u \exp(i\theta_2) + a_W^u \exp(-i\theta_1) + a_S^u \exp(-i\theta_2)]\}$$
$$= \tilde{\alpha}_\theta^u\{a_P^u + r_{mom}[a_E^u \exp(i\theta_1) - a_P^u]\} - \frac{4r_{mom}\mu_0}{h^2}\alpha_\theta^v s_1 s_2 - \frac{2r_{mom}i}{h}\alpha_\theta^p s_1. \tag{26}$$

So for the total alternating sweep we have

$$\dot{\alpha}_\theta^u = \frac{1}{\eta_x^u \eta_y^u}[v_x^u v_y^u \alpha_\theta^u - (\eta_x^u + v_y^u)(\varphi\alpha_\theta^v + \zeta^u \alpha_\theta^p)], \tag{27}$$

where

$$\varphi = \frac{4r_{mom}\mu_0}{h^2}s_1 s_2, \qquad \zeta^u = \frac{2r_{mom}i}{h}s_1,$$

$$\eta_x^u = a_P^u - r_{mom}[a_E^u \exp(i\theta_1) + a_W^u \exp(-i\theta_1) + a_S^u \exp(-i\theta_2)],$$
$$\eta_y^u = a_P^u - r_{mom}[a_N^u \exp(i\theta_2) + a_W^u \exp(-i\theta_1) + a_S^u \exp(-i\theta_2)],$$
$$v_x^u = a_P^u + r_{mom}[a_N^u \exp(i\theta_2) - a_P^u],$$
$$v_y^u = a_P^u + r_{mom}[a_E^u \exp(i\theta_1) - a_P^u].$$

The v-momentum relaxation follows along similar lines and leads to the amplification

$$\dot{\alpha}_\theta^v = \frac{1}{\eta_x^v \eta_y^v}[v_x^v v_y^v \alpha_\theta^v - (\eta_x^v + v_y^v)(\varphi\dot{\alpha}_\theta^u + \zeta^v \alpha_\theta^p)], \tag{28}$$

where

$$\zeta^v = \frac{2r_{mom}i}{h}s_2,$$

$$\eta_x^v = a_P^v - r_{mom}[a_E^v \exp(i\theta_1) + a_W^v \exp(-i\theta_1) + a_S^v \exp(-i\theta_2)],$$
$$\eta_y^v = a_P^v - r_{mom}[a_N^v \exp(i\theta_2) + a_W^v \exp(-i\theta_1) + a_S^v \exp(-i\theta_2)],$$
$$v_x^v = a_P^v + r_{mom}[a_N^v \exp(i\theta_2) - a_P^v],$$
$$v_y^v = a_P^v + r_{mom}[a_E^v \exp(i\theta_1) - a_P^v].$$

Thus the first stage of the SIMPLE pressure-correction algorithm amplifies the $\boldsymbol{\theta}$ error components as follows:

$$\begin{bmatrix} 1 & 0 & 0 \\ \dfrac{\varphi}{\eta_x^v \eta_y^v}(\eta_x^v + v_y^v) & 1 & 0 \\ 0 & 0 & 1 \end{bmatrix} \begin{bmatrix} \dot{\alpha}_\theta^u \\ \dot{\alpha}_\theta^v \\ \dot{\alpha}_\theta^p \end{bmatrix} = \begin{bmatrix} \dfrac{v_x^u v_y^u}{\eta_x^u \eta_y^u} & -\dfrac{\varphi}{\eta_x^u \eta_y^u}(\eta_x^u + v_y^u) & -\dfrac{\zeta^u}{\eta_x^u \eta_y^u}(\eta_x^u + v_y^u) \\ 0 & \dfrac{v_x^v v_y^v}{\eta_x^v \eta_y^v} & -\dfrac{\zeta^v}{\eta_x^v \eta_y^v}(\eta_x^v + v_y^v) \\ 0 & 0 & 1 \end{bmatrix} \begin{bmatrix} \alpha_\theta^u \\ \alpha_\theta^v \\ \alpha_\theta^p \end{bmatrix} \tag{29}$$

From equation (29) the amplification matrix $\mathbf{A}_1$ of the momentum relaxation stage of the SIMPLE algorithm is easily calculated. As an alternative—at high Reynolds numbers—an alternating *symmetric* line SOR method could be used. This would ensure that at some stage during the momentum relaxation the equations are being swept in a downstream direction, which may be beneficial to the smoothing rate. The calculation of the relevant amplification matrix $\mathbf{A}_1$ in this case is straightforward, following exactly the same principles outlined above.

Pressure correction

With reference to Figure 1, the pressure correction proceeds as follows:

$$\ddot{u}_P = \dot{u}_P - \frac{r_{uv}}{a_P^u h}(\delta p_P - \delta p_W), \tag{30}$$

$$\ddot{v}_P = \dot{v}_P - \frac{r_{uv}}{a_P^v h}(\delta p_P - \delta p_S), \tag{31}$$

$$\ddot{p}_P = \dot{p}_P + r_p \delta p_P, \tag{32}$$

where r_{uv} and r_p are relaxation parameters for updating velocities and pressure respectively. δp is an approximation to the solution of an equation

$$a_P^p \delta p_P = a_N^p \delta p_N + a_S^p \delta p_S + a_E^p \delta p_E + a_W^p \delta p_W - \frac{1}{h}(\dot{u}_E - \dot{u}_P + \dot{v}_N - \dot{v}_P), \tag{33}$$

$$a_N^p = \frac{1}{a_P^v h^2} = a_S^p, \qquad a_E^p = \frac{1}{a_P^u h^2} = a_W^p, \qquad a_P^p = \sum_\alpha a_\alpha^p,$$

α ranging over N, S, E, W points.

Writing equation (33) as

$$P_h \delta p_h = \delta_h^x \dot{u}_h + \delta_h^y \dot{v}_h, \tag{34}$$

(30)–(32) as

$$\ddot{u}_h = \dot{u}_h - \frac{r_{uv}}{a_P^u} \delta_h^x \delta p_h, \tag{35}$$

$$\ddot{v}_h = \dot{v}_h - \frac{r_{uv}}{a_P^v} \delta_h^y \delta p_h, \tag{36}$$

$$\ddot{p}_h = \dot{p}_h + r_p \delta p_h \tag{37}$$

and substituting (34) into (35)–(37), we have

$$\ddot{u}_h = \dot{u}_h - \frac{r_{uv}}{a_P^u} \delta_h^x P_h^{-1}(\delta_h^x \dot{u}_h + \delta_h^y \dot{v}_h), \tag{38}$$

$$\ddot{v}_h = \dot{v}_h - \frac{r_{uv}}{a_P^v}\delta_h^y P_h^{-1}(\delta_h^x \dot{u}_h + \delta_h^y \dot{v}_h), \tag{39}$$

$$\ddot{p}_h = \dot{p}_h + r_p P_h^{-1}(\delta_h^x \dot{u}_h + \delta_h^y \dot{v}_h) \tag{40}$$

(assuming that (34) has been solved exactly). The true solution clearly satisfies relations such as (38)–(40) and so the errors may be written as

$$\ddot{e}_h^u = \dot{e}_h^u - \frac{r_{uv}}{a_P^u}\delta_h^x P_h^{-1}(\delta_h^x \dot{e}_h^u + \delta_h^y \dot{e}_h^v), \tag{41}$$

$$\ddot{e}_h^v = \dot{e}_h^v - \frac{r_{uv}}{a_P^v}\delta_h^y P_h^{-1}(\delta_h^x \dot{e}_h^u + \delta_h^y \dot{e}_h^v), \tag{42}$$

$$\ddot{e}_h^p = \dot{e}_h^p + r_p P_h^{-1}(\delta_h^x \dot{e}_h^u + \delta_h^y \dot{e}_h^v). \tag{43}$$

Substituting Fourier components as before, we obtain

$$\begin{bmatrix} \ddot{\alpha}_\theta^u \\ \ddot{\alpha}_\theta^v \\ \ddot{\alpha}_\theta^p \end{bmatrix} = \begin{bmatrix} 1 + \dfrac{4r_{uv}s_1^2}{a_P^u \hat{P}_h(\boldsymbol{\theta})h^2} & \dfrac{4r_{uv}s_1 s_2}{a_P^u \hat{P}_h(\boldsymbol{\theta})h^2} & 0 \\ \dfrac{4r_{uv}s_1 s_2}{a_P^v \hat{P}_h(\boldsymbol{\theta})h^2} & 1 + \dfrac{4r_{uv}s_2^2}{a_P^v \hat{P}_h(\boldsymbol{\theta})h^2} & 0 \\ \dfrac{2r_p s_1}{h\hat{P}_h(\boldsymbol{\theta})}\mathrm{i} & \dfrac{2r_p s_2}{h\hat{P}_h(\boldsymbol{\theta})}\mathrm{i} & 1 \end{bmatrix} \begin{bmatrix} \dot{\alpha}_\theta^u \\ \dot{\alpha}_\theta^v \\ \dot{\alpha}_\theta^p \end{bmatrix}, \tag{44}$$

where $\hat{P}_h(\boldsymbol{\theta})$ is the symbol of P_h:

$$\hat{P}_h(\boldsymbol{\theta}) = a_E^p \exp(\mathrm{i}\theta_1) + a_W^p \exp(-\mathrm{i}\theta_1) + a_N^p \exp(\mathrm{i}\theta_2) + a_S^p \exp(-\mathrm{i}\theta_2) - a_P^p.$$

Thus the amplification matrix $\mathbf{A}_2$ of the pressure-correction stage of the SIMPLE algorithm is defined by (44).

Smoothing factors

The smoothing factor of the SIMPLE algorithm is calculated as follows. The amplification matrix $\mathbf{A} = \mathbf{A}_2\mathbf{A}_1$ is easily calculated from equations (29) and (44). $\mathbf{A}$ is a 3×3 complex non-Hermitian matrix. Its amplification factor $\mu(\boldsymbol{\theta}) = \rho(\mathbf{A})$ is found using a NAG routine for the eigenvalues of a general matrix. The smoothing factor defined by equation (20) is then found by embedding the calculation of $\mu(\boldsymbol{\theta})$ in a NAG routine for linearly constrained minimization. The definition of $\bar{\mu}$ for highly convective flow given in equation (21) was found to be too costly to evaluate. As an alternative we define the smoothing factor to be

$$\bar{\mu} = \max_{(u_0,v_0)\in\mathscr{U}} \left\{ \sup_{\theta\in\mathscr{H}} [\rho(\mathbf{A})] \right\}, \tag{45}$$

where $\mathscr{U} = \{(0,1), (1,1), (1,0), (1,-1), (0,-1), (-1,-1), (-1,0), (-1,1)\}$ is a set of flow directions of interest.

Smoothing factors are presented in graphical format in Figures 2–12. Two different styles of presentation are employed. Figures 2–6 show contours and isometric plots of the amplification factors at various mesh Reynolds numbers and flow directions. The contour k gives a value $\mu(\boldsymbol{\theta}) = k/10$. A good smoother should have a small amplification factor in the high-frequency region of the $\boldsymbol{\theta}$ plane: $(\theta_1, \theta_2) \in \mathscr{H} = [-\pi, \pi]^2/(-\pi/2, \pi/2)^2$.

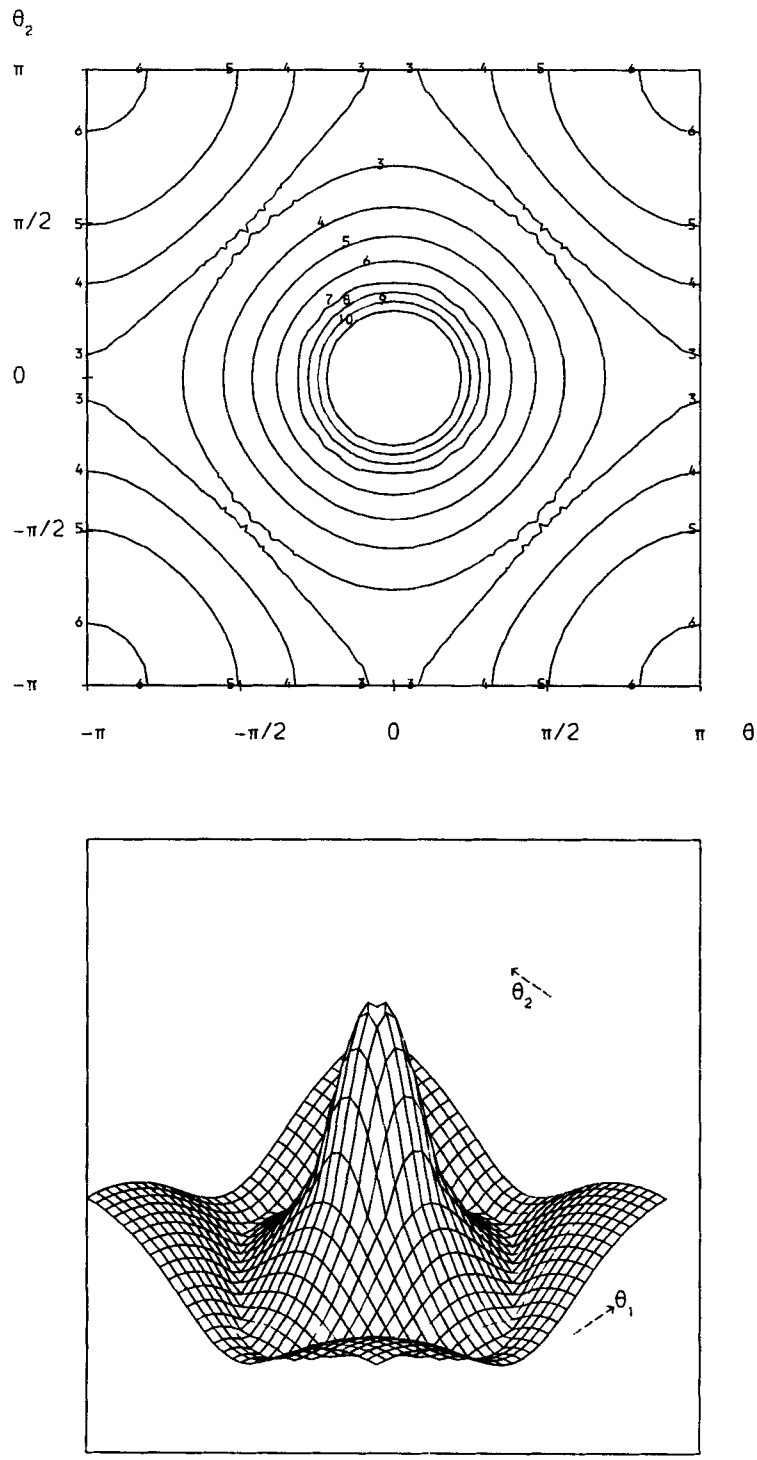

Figure 2. Amplification factor at mesh Reynolds number 1

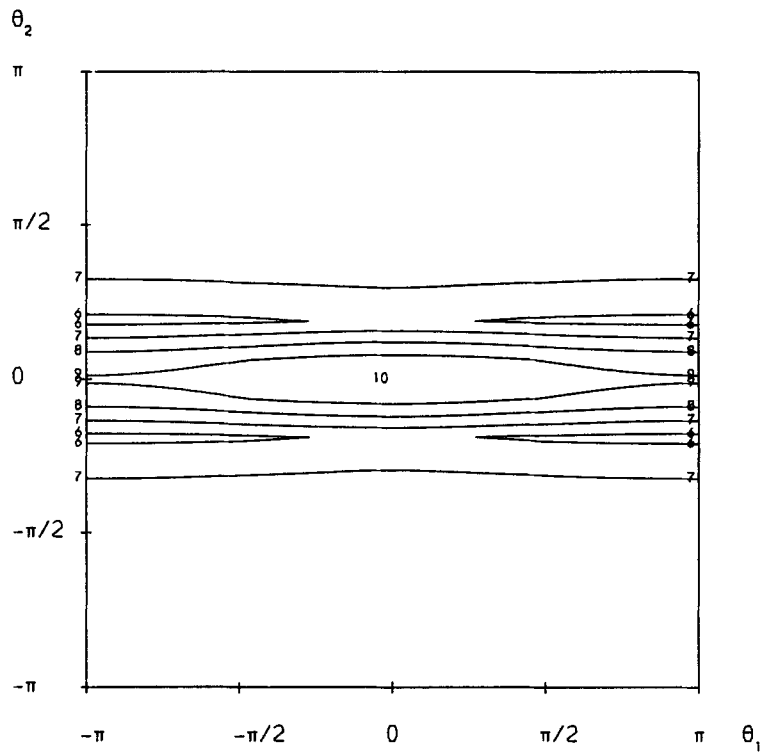

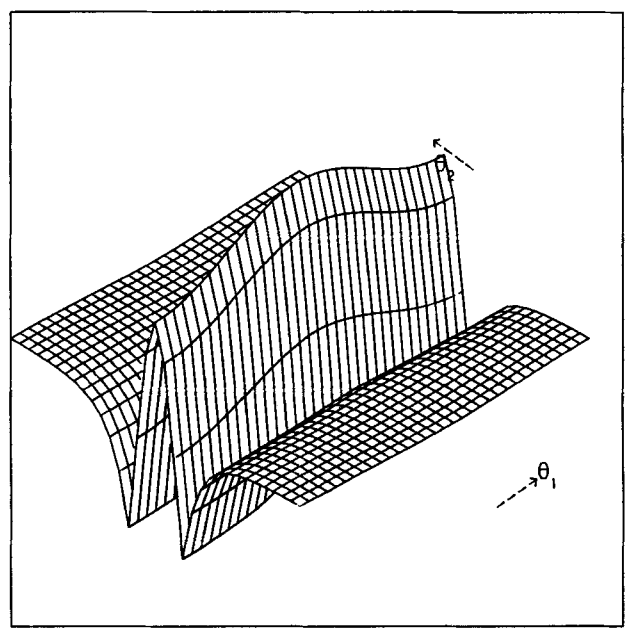

Figure 3. Amplification factor at mesh Reynolds number 100; $(u_0, v_0) = (0, 1)$

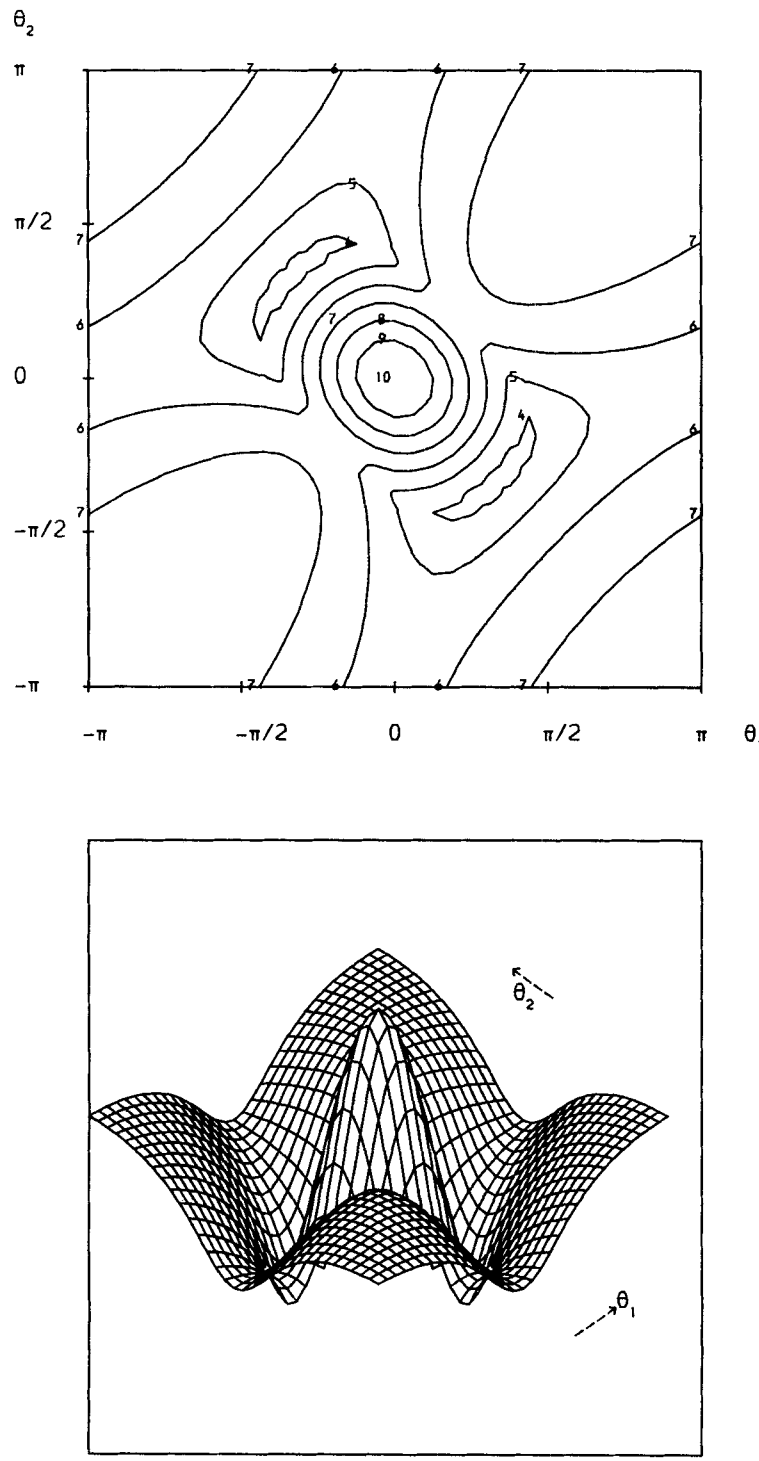

Figure 4. Amplification factor at mesh Reynolds number 100; $(u_0, v_0) = (1, 1)$

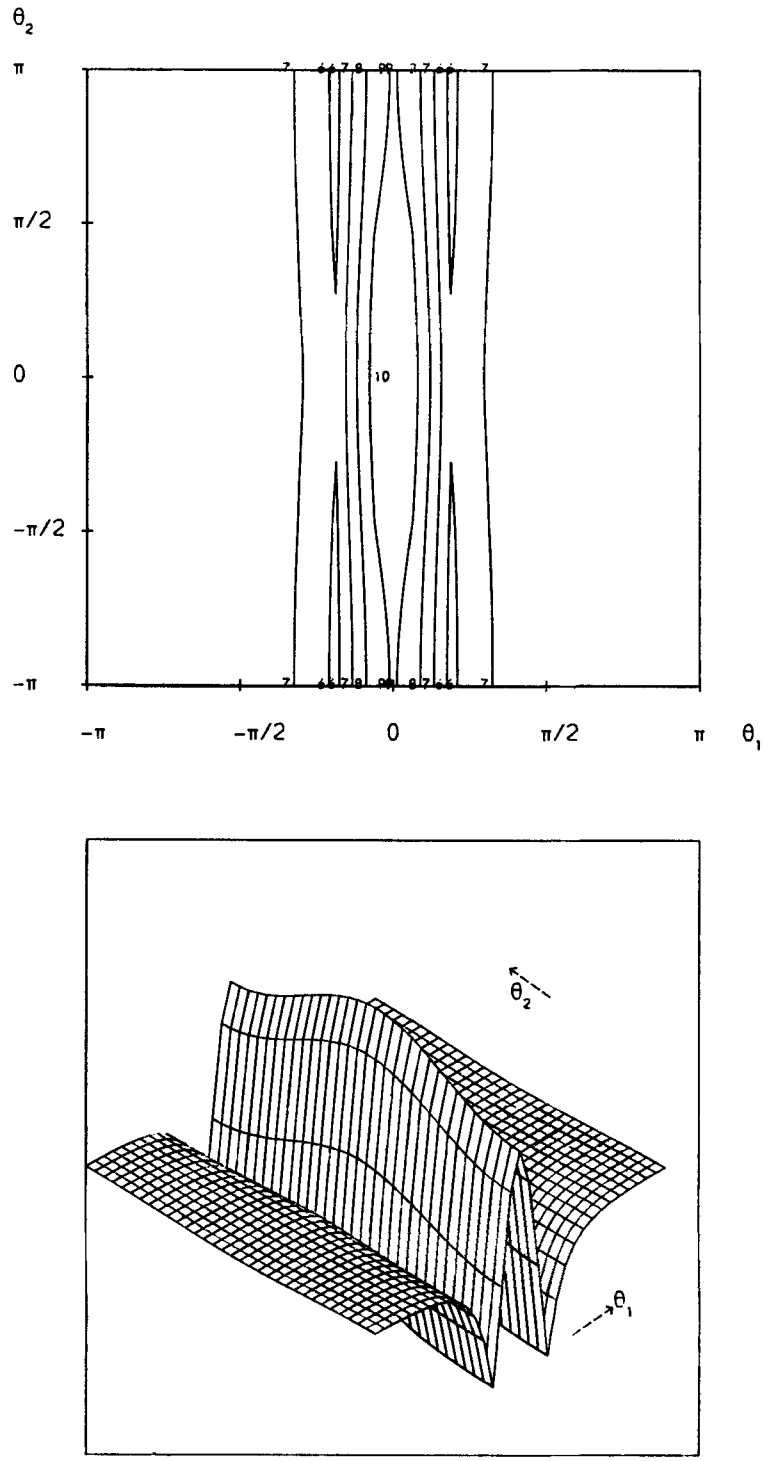

Figure 5. Amplification factor at mesh Reynolds number 100; $(u_0, v_0) = (1, 0)$

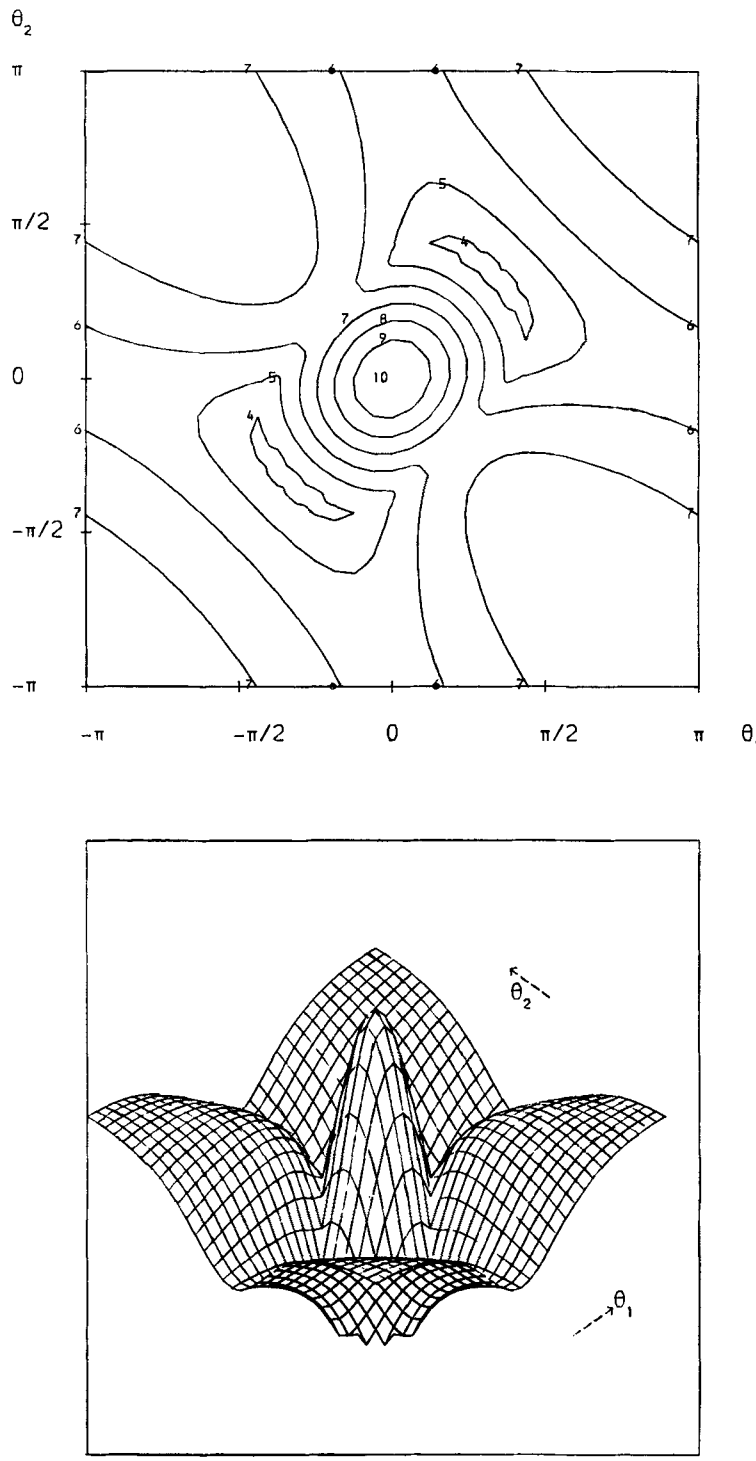

Figure 6. Amplification factor at mesh Reynolds number 100; $(u_0, v_0) = (1, -1)$

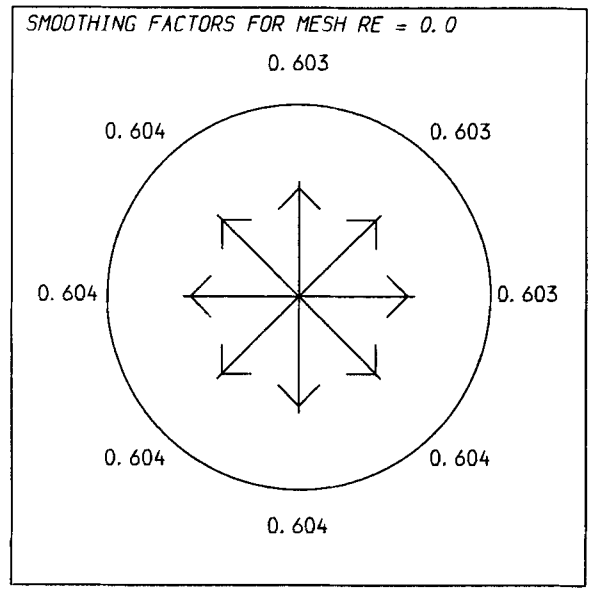

Figure 7. $\bar{\mu}$ for velocities in $\mathscr{U}$ at $Re = 1$

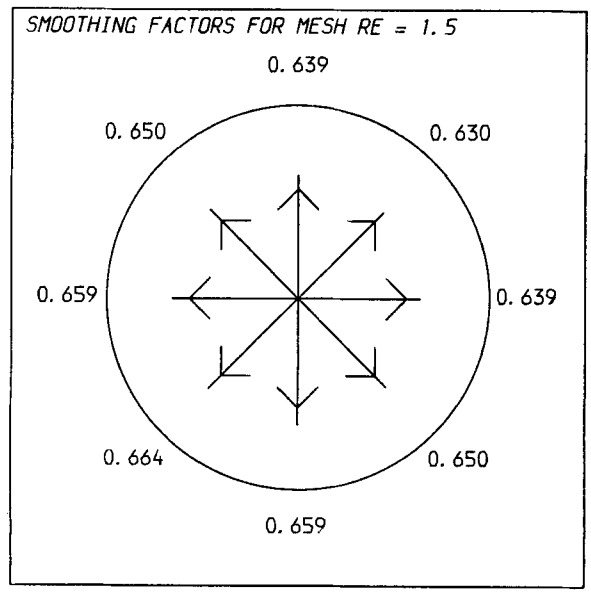

Figure 8. $\bar{\mu}$ for velocities in $\mathscr{U}$ at $Re = 100$

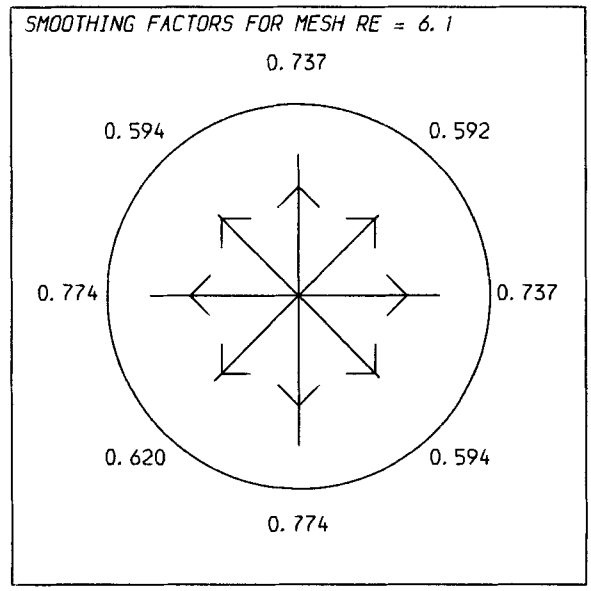

Figure 9. $\bar{\mu}$ for velocities in $\mathscr{U}$ at $Re = 400$

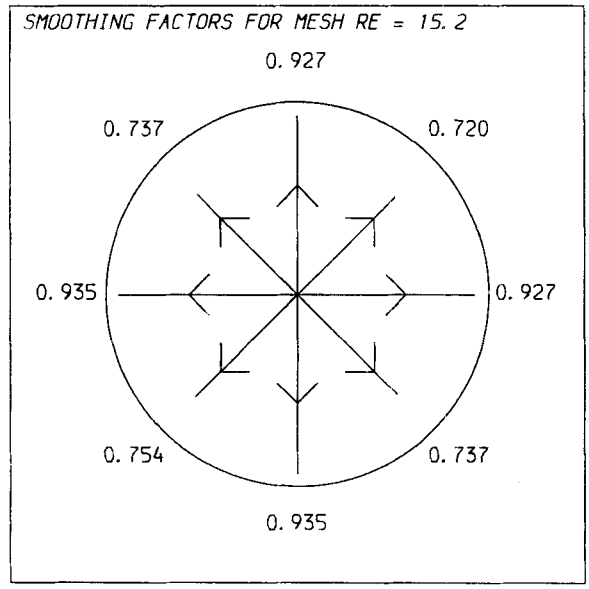

Figure 10. $\bar{\mu}$ for velocities in $\mathscr{U}$ at $Re = 1000$

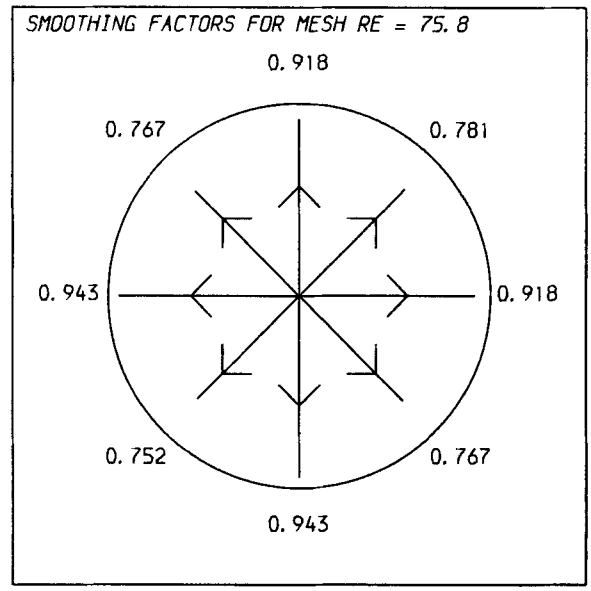

Figure 11. $\bar{\mu}$ for velocities in $\mathscr{U}$ at $Re = 5000$

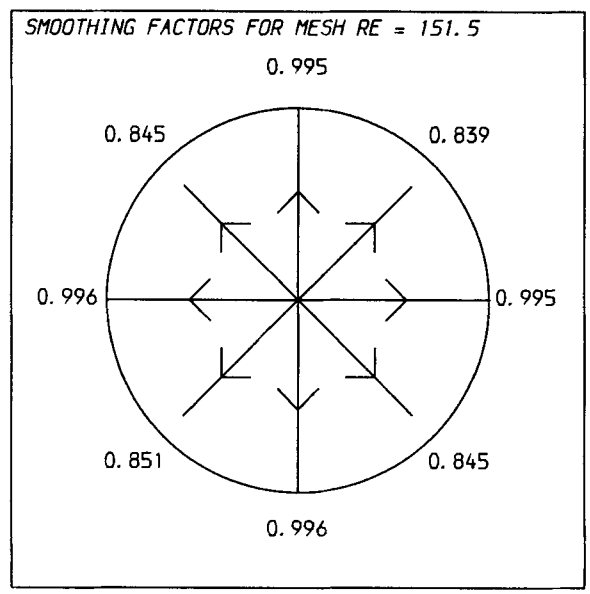

Figure 12. $\bar{\mu}$ for velocities in $\mathscr{U}$ at $Re = 10000$

Figures 7–12 show $\bar{\mu}$ as defined by equation (20) for the flow directions in the set $\mathscr{U}$. The Reynolds numbers tested are those used in Sivaloganathan and Shaw.[1] In the next section these factors will be compared with experimental convergence results. Each arrow points in the relevant direction in (u_0, v_0) space. The length of the arrow in that flow direction is proportional to $\bar{\mu}$ for that velocity. Desirable features of $\bar{\mu}$ are that it should be bounded reasonably below unity and that it should be fairly independent of flow direction.

The relaxation factors $r = \{r_{\text{mom}}, r_{uv}, r_p\}$ used in Figures 2–6 are given in Table I together with the smoothing factors obtained. In these cases the analysis assumes that alternating *symmetric* line SOR has been used for the momentum equations. Table II gives similar results for Figures 7–12, listing the minimum and maximum values of $\bar{\mu}$ obtained over all flow directions in $\mathscr{U}$. These results are for *unsymmetric* alternating SOR in correspondence with the practical experiments.

Figure 2 shows the amplification factor at mesh Reynolds number 1 for a flow direction $(u_0, v_0) = (0, 1)$. The smoothing factor in this case is $\bar{\mu} = 0{\cdot}619$. At such a low mesh Reynolds number the amplification factor is independent of flow direction. Clearly SIMPLE is a satisfactory smoother for diffusion-dominated flows.

In Figures 3–6 the same information is depicted for convection-dominated flow at mesh Reynolds number 100. The flow direction for each figure is $(0, 1)$, $(1, 1)$, $(1, 0)$ and $(1, -1)$ respectively. Owing to symmetry of the amplification factor, the contours for all other members of $\mathscr{U}$ are identical to one of these. The discrete ellipticity analysis showed that the imaginary part of the symbol of the discrete operator becomes zero along lines in the $\boldsymbol{\theta}$ plane which are perpendicular to the flow direction. Discrete ellipticity is most nearly lost along such lines. As suggested, this has a marked effect on the amplification factor at high mesh Reynolds numbers. This is illustrated admirably in Figures 3–6. In Figure 3 the amplification is clearly largest along the line $\theta_2 = 0$, which is perpendicular to the flow direction $u_0 = 0$. In Figure 4 this maximum

Table I. Relaxation factors and smoothing (factors for Figures 2–6). In all cases $r_{uv} = 1 = r_p$

Figure	r_{mom}	$\bar{\mu}$
2	0·42	0·619
3	0·15	0·993
4	0·15	0·839
5	0·15	0·993
6	0·15	0·845

Table II. Relaxation factors and smoothing (factors for Figures 7–12). In all cases $r_{uv} = 1 = r_p$

Figure	r_{mom}	$\bar{\mu}_{\text{min}}$	$\bar{\mu}_{\text{max}}$
7	0·50	0·603	0·604
8	0·45	0·630	0·664
9	0·40	0·592	0·774
10	0·25	0·720	0·935
11	0·15	0·839	0·992
12	0·15	0·839	0·996

has moved to the line $\theta_1 = -\theta_2$, in Figure 5 to $\theta_1 = 0$ and in Figure 6 to $\theta_1 = \theta_2$. In all cases it is perpendicular to the flow direction. These poor smoothing rates at high mesh Reynolds numbers along such lines in the $\boldsymbol{\theta}$ plane are a feature of the discretization—which nearly loses ellipticity—rather than the SIMPLE algorithm. Any algorithm applied to the discretization (10) will yield poor smoothing rates along these lines. Furthermore, a more suitable discretization is not available without the use of extra stabilizing terms (artificial viscosity). However, some improvement in smoothing factors may be obtained by judicious choice of the relaxation factor r.

Figures 7–12 show smoothing factors for the set of velocities $(u_0, v_0) \in \mathscr{U}$ as described above. The Reynolds numbers for these figures are 1, 100, 400, 1000, 5000 and 10000 respectively. These and the mesh length $h = 1/66$ are chosen in accordance with the practical experiments of Sivaloganathan and Shaw.[1] The corresponding mesh Reynolds number appears at the top of each figure. As can be seen from Figures 7 and 8, the SIMPLE algorithm is a good smoother up to $Re = 100$, with $\bar{\mu}$ ranging from 0·604 to 0·664 and little variation due to flow direction. For these cases the mesh Reynolds number is less than 2 and hence from equations (7) and (8) of Sivaloganathan and Shaw[1] we see that the upwind differencing has not come into effect. At $Re = 400$ the influence of the flow direction begins to show, but the algorithm is still a good smoother with $\bar{\mu} = 0{\cdot}774$. From $Re = 1000$ to $Re = 10000$ the flow direction bcomes more important still and the smoothing rates are poorer, albeit principally along particular lines in the $\boldsymbol{\theta}$ plane. These rates may be improved by the choice of r. In considering smoothing analysis at high Reynolds numbers it should be remembered that the linearization made in the analysis is less valid than for diffusion-dominated flow. The main aim of such an analysis should therefore be to show that a method behaves well for moderate Reynolds number. It is clear that SIMPLE satisfies this criterion.

A COMPARISON OF THEORETICAL AND PRACTICAL SMOOTHNG ANALYSIS

As mentioned at the end of the previous section, some doubt exists as to the validity of the theoretical smoothing analysis in the case of convection-dominated flow. This is principally due to the linearization, which assumes a constant velocity field when evaluating non-linear terms in equations (1). In practice these velocities are locally variable and dependent on the current solution.

Given a multigrid method for solution of the problem under consideration, a practical smoothing analysis may be made in order to test the validity of the theoretical analysis. This is possible since the theoretical smoothing factor is defined to be the asymptotic convergence rate of each smoothing iteration in a two-grid multigrid method with a perfect coarse grid correction; i.e., a coarse grid correction which annihilates all error components in the 'low'-frequency range $\boldsymbol{\theta} \in \mathscr{L} = (-\pi/2, \pi/2)^2$. For more details of this interpretation of the smoothing factor see Stüben and Trottenberg.[10]

It is not difficult to simulate this type of method in practice. A multigrid method is used to solve the problem on a finest grid denoted by Ω_m. Progressively coarser grids Ω_k, $k = m - 1(-1)1$ are defined in a natural manner. The multigrid method used has ν_1 pre-relaxations, ν_2 post-relaxations and γ_k coarse grid corrections on each grid $\Omega_k \cdot \gamma_m$ is chosen to be 1, as in a conventional multigrid method (where $\gamma = 1$ or $\gamma = 2$ are the usual choices). γ_{m-1} is chosen to be much larger, so that the coarse grid correction for Ω_m is solved almost exactly. On coarser grids $\gamma_k = 1$, $k = m - 2(-1)1$ is a reasonable definition. This method simulates the situation described

Table III. Theoretical and practical smoothing factors

Reynolds	$\bar{\mu}_{min}$	$\bar{\mu}_{max}$	$\bar{\mu}_p$
1	0·603	0·604	0·478
100	0·630	0·664	0·558
400	0·592	0·774	0·588
1000	0·720	0·935	0·725
5000	0·839	0·992	0·840
10000	0·839	0·996	0·910

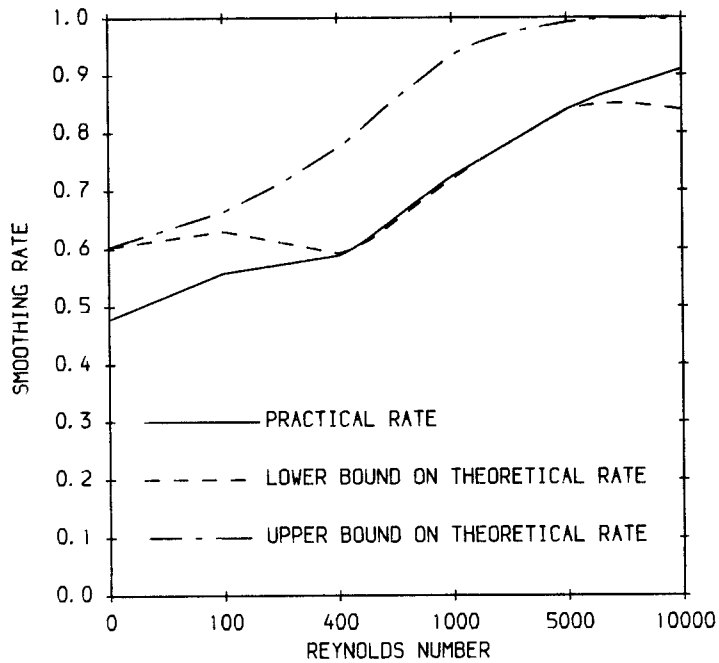

Figure 13. Comparison of theoretical and practical smoothing rates

above. The practical smoothing factor $\bar{\mu}_p$ is therefore defined by

$$\bar{\mu}_p = (\kappa_{mg})^{1/(\nu_1+\nu_2)}, \tag{46}$$

where κ_{mg} is the asymptotic convergence rate of the multigrid method described above. If the theoretical analysis is valid, $\bar{\mu}$ and $\bar{\mu}_p$ will be in close agreement.

Table III gives values of $\bar{\mu}_p$ for the experiments described in Sivaloganathan and Shaw[1] together with minimum and maximum theoretical smoothing rates over velocity fields in $\mathscr{U}$. These three rates are also depicted in Figure 13. It is clear that the minimum theoretical smothing rate accurately models the practical behaviour of SIMPLE as a smoothing method, even for high Reynolds numbers. Note from Figures 9–12 that $\bar{\mu}_{max}$ always occurs for velocity fields aligned with grid lines. For practical flows in which there is no persistent alignment between streamlines and grid lines one would therefore expect the method to behave as predicted by $\bar{\mu}_{min}$. This indeed seems to be the case for the present recirculating flow problem—shear-driven cavity. However, even in

cases of strong alignment $\bar{\mu}_{max}$ is expected to be a pessimistic prediction of the practical smoothing rate.

Figure 13 also demonstrates the divergence of the two theoretical rates which occurs at the onset of upwinding—at mesh Reynolds number 2, corresponding to Reynolds number 132.

CONCLUSIONS

A theoretical analysis of the smoothing capabilities of the SIMPLE pressure correction has been presented. This analysis has shown that h-independent convergence rates are attainable by a multigrid method for solution of the incompressible Navier–Stokes equations. Such convergence rates have already been achieved in practice.

The analysis has been compared with the practical behaviour of the method and found to be an accurate predictor of convergence rates.

The potential for improvement of the existing method by further analysis of the theoretical results is enormous. For example, optimization of the smoothing rate with respect to the relaxation parameters is one possible avenue. The analysis presented also permits a critical evaluation of candidate smoothers, since it is readily adapted for application to modified pressure-correction schemes such as SIMPLER and SIMPLEST.

ACKNOWLEDGEMENTS

The authors would like to thank the SERC and Rolls–Royce, PLC for financial support during the course of this research.

REFERENCES

1. S. Sivaloganathan and G. J. Shaw, 'A multigrid method for recirculating flows', *Int. j. numer. methods fluids*, **7**, 417–440 (1987).
2. S. V. Patankar and D. B. Spalding, 'A calculation procedure for heat and mass transfer in 3-D parabolic flows', *Int. J. Heat Mass Transfer*, **15**, 1787–1806 (1972).
3. A. Douglis and L. Nirenberg, 'Interior estimates for elliptic systems of partial differential equations', *Comm. Pure Appl. Math.*, **8**, 503–538 (1955).
4. V. Thomée, 'Elliptic difference operators and Dirichlet problems', *Contrib. Diff. Equations*, **3**, 301–324 (1964).
5. A. Brandt and N. Dinar, 'Multigrid solutions to elliptic flow problems', in S. V. Parter (ed.), *Numerical Methods for PDEs*, Academic Press, New York, 1979, pp. 53–147.
6. G. J. Shaw, 'Multigrid methods in fluid dynamics', *D. Phil. Thesis*, Oxford University, 1985.
7. P. W. Hemker, 'Fourier analysis of gridfunctions, prolongations and restrictions', *Preprint NW 93/80*, Department of Numerical Mathematics, Mathematical Centre, Amsterdam, 1980.
8. A. Brandt, 'Numerical stability and fast solutions of boundary value problems', in J. J. H. Miller (ed.), *Boundary and Interior Layers–Computational and Asymptotic Method*, Boole Press, Dublin, 1980, pp. 29–49.
9. A. Brandt, 'Multi-level adaptive solutions of boundary value problems', *Math. Comput.*, **31** (138), 333–390 (1977).
10. K. Stüben and U. Trottenberg, 'Multigrid methods: fundamental algorithms, model problem analysis and applications', *Lecture Notes in Mathematics*, **960**, Springer-Verlag, New York, 1981, pp. 1–176.